COMPARATIVE DESIGN AND CFD ANALYSIS OF 3-D PRINTED ACRYLONITRILE BUTADIENE STYRENE NOZZLE AERATOR FOR DISCHARGE REDUCTION

by

Bovas Herbert Bejaxhin ALPHONSE[a], Ramji BASAVARAJ RAYAPPA[b], Hasan KOTEN[c], Ramesh BALASUBRAMANIAN[d], and Deepak UMRAO SARWE[e]*

[a]Department of Mechanical Engineering, Saveetha School of Engineering,
Saveetha Institute of Medical and Technical Sciences, Chennai, Tamil Nadu, India
[b]Department of Industrial Engineering and Management, B.M.S. College of Engineering, Bengaluru,
Karnataka, India
[c]Mechanical Engineering Department, Istanbul Medeniyet University, Goztepe Campus,
Istanbul Turkey
[d]Institute of Mechanical Engineering, Saveetha School of Engineering,
Saveetha Institute of Medical and Technical Sciences, Chennai, Tamil Nadu, India
[d]Department of Mathematics, University of Mumbai, Kalina, Santacruz,
East Mumbai, Maharashtra, India

The flow nozzle aerator, which is the part of the water tap made up of acrylonitrile butadiene styrene, can be modified entirely with a new design. The curved and cone-shaped slopes are used to improve the smooth flow at uniform velocity. Simultaneously, discharge is optimum by modified interior design. The smooth laminar delivery of water with optimum pressure, the liquid element at the aerator end becomes smooth. The assembled nozzle aerator solid model has been generated before experimentation. This can promote through the prediction by the modern tool ANSIFLUENT and CFD for finding the flow behavior and its outlet characters. The solid model can be fabricated to prototype for accurate dimensions by using 3-D printing technology. Comparing fluid motion with the time consumption of filling water has been done over these different kinds of aerator and nozzle models, which are fabricated by 3-D printing.

Keywords*: 3-D printing, aerator, CFD, flow rate, nozzle; velocity*

Introduction

In recent days, a considerable amount of water was consumed unwantedly by the human environment for domestic purposes and industries. In nature, the groundwater levels and running streams reduced in its flow rate due to a lot of global changes. The lag of water flows in the tap outlet due to clogging, the formation of sediments inside the tap nozzle, and debris efficiently slow down the water supply to a dribble. Some of the kids played by opening the tap to waste out the water without any control. So these kinds of issues were raised due to the usage of irregularly shaped nozzles and its aerators. By replacing this kind of enormous water usage, we could introduce the nozzle aerator for water tap assembly setup in

---

*Corresponding author, e-mail: herbert.mech2007@gmail.com

our routine applications. Its main objective is to reduce the water consumption by the innovative flow nozzle, which can use to compare the discharge level and flow velocity by using various design of flow nozzle and accessories. It can achieve up to 90% and above water savings, which will be persistent for future generations and also encourages the CFD analysis for easy prediction of flow results before the manufacture of nozzles and pipeline products with the consideration of losses. The rapid manufacturing of 3-D printings helps to renovate the product; whatever we need it for the analysis of model and flow characteristics. Based on AECB European water level standards (2013), the water-efficient taps can be used in the kitchens for cookery purposes, with the flow rates of 4-6 Lpm has been denoted. Similarly, the bathroom taps and sprays levels up to 6 Lpm flow rates can be maintained. Rahi *et al*. [1] have discussed the comparison of experimental and numerical analysis of minor losses, and the loss minimization techniques have verified over the concentric pipes, which had uneven cross-sections. The turbulent eddies in different pipelines' corner areas create energy loss due to sudden contraction and expansion. The changes in its cross-sectional area have changed the velocity due to the different diameters of pipelines. Pandey *et al*. [2] has been verified and validated that the effect of flow angles made much influence on the various flow properties, and its behavior of the compressor cascade could be analyzed. The curved distortion of the blades leads to better performance of the gas turbine.

Liu *et al*. [3] have discussed that the analytical results compared with the experimental values of finding the error percentages that the solutions were consistent with the experimental results. The influencing factors on the pressure distribution along this perforated pipes by the factors friction and momentum. The changes in slope and the adjustments of length to diameter with the participation of the Reynolds number used to regulate the dominants of gravity, energy, and friction. The discharge from the different holes becomes the same due to hydrodynamic pressure distribution. Baghdadi *et al*. [4] discussed the experimental verification of leakage location of pipes in the circular and rectangular cross-sectional tubes with more turbulent in nature the developed mathematical model with the theoretical method used to locate the leakages. Ahmed *et al*. [5] have discussed that the predicted results of velocity distribution, the pressure drop in a pipeline have mentioned the unsymmetrical solid particle distributions along the vertical plane of the pipelines due to the influence of turbulent energy. At the higher efflux concentration, the pipe wall increased by the interaction of solid particles with higher velocities.

Tartibu *et al*. [6] discussed the velocity distribution of flow streaming of one rounded, and one rectangular stack edge profile was analyzed. If the drive ratio of the flow pathlines increased, the non-linear effect and the discrepancies have observed. Farsirotou *et al*. [7] have discussed that the minor losses incorporated in the incompressible fluid-flow pipelines because of various pipe fittings and accessories. It has observed from the experimental values that the higher mass-flow rate have been created more minor head losses due to cross-sectional changes. Vijayan *et al*. [8] have described the CFD simulation of two-phase fluid movement inside a modified vapour separator has carried out using COSMOS EXPRESS software package. The drawbacks and effects of turbulence and pressure drop on the existing vapour separator design have studied to improve the efficiency levels. Adel *et al*. [9] have discussed that the standard aeration efficiency (SAE) has increased concerning to the impeller's rotational speed. The maximum SAE achieved if the number of impeller blades increased and reduced due to the quick increase of input power. Wang *et al*. [10] have discussed the laminar flow can be analyzed based on some simulation results of velocity contours and vectors over the different shaped ribs. These ribs delightfully increased by the local heat transfer,

and friction performance at the ribs' windward side has identified. They found that the trapezoidal rib showed the best performance with the Reynolds Number ranging from 100-900. Shukla *et al*. [3] discussed that the increase in the number of openings and the increase in total surface area of openings used to elevate the discharge with the increase in oxygen transfer coefficient.

Jahan *et al*. [12] evaluated that the same cooling time has identified for the cooling time of design case studies for both the circular and rectangular channels. The average displacements on the core area become less compare with the cavity for design cases that have verified. Kamel *et al*. [13] have discussed the investigation of two-phase flow simulations of nanofluids or vapour in the rectangular boiling chamber, which showed that the more significant could be identified as volume fraction in pure water than the silica-based nanowater for a given value of superheat temperature. The heating surface can attribute the deposition of nanoparticles during the boiling process can be identified. Jafari *et al*. [14] have discussed that the porous structure created by the 3-D model can be utilized by measuring the capillary rise and permeability of the fluid-flow. Due to the gravitational effect and the slower capillary growth, they played a significant role in the 3-D printed wick, and the SEM characterization can identify it. It has confirmed that the permeability becomes more by the performance of a 3-D printed heat pipe can significantly enhance the heat transfer. Lorinczy *et al*. [15] have discussed that the biomedical applications will benefit from colossal product development through this 3-D printing. Using nanoparticulate antibacterial materials can be used to develop new products in the field of biomedical applications. Surgical oriented devices and filaments have made by using PLA-HDT and PLA-Ag with silver nanoparticles fibres. For the more temperature range, the thermal characteristics of PLA-Ag and 3-D printed nanoparticles have identified, resulting in excellent response and minimization of antibacterial effect and infections in the heat-based sterilization methods usage of 3-D printed materials.

Naresh *et al*. [16] have accomplished by the analysis over the geometric features of the impeller of the mixed flow pump, which used to identify the effect of various designs and operating parameters of the pump blade impeller by the CFD method of analysis. The predicted values of pressure and velocities in the outlet distribution are beneficial for identifying the pump's excellent efficiency. Guo *et al*. [17] have outlined the graphane based composites which were made by the 3-D printing techniques with effective simulation and characterization methods to take part in developing new products, either regular or nanosized applications. The DIW and GO-based methods of 3-D printing are advisable, and it stoutly depended on the inherent properties of different materials. Due to the highly precise and resolution, the SLA method has also recommended. Kumar *et al*. [18] have discussed that the achievement of subsonic velocity at the outlet in the form of non-axisymmetric air-foil rectangular nozzle by conducting the types of fluid-flows and thermal characteristics on the nozzle geometry. It can assist with the conduction of CFD simulations, and the flow variations of different gases with specific pressures have verified with the 3-D cell configurations of CFD analysis. The maximum velocity, which was influenced by its density, can be achieved by the lesser density gasses while at cryogenic temperatures. Bhowmick *et al*. [19] have discussed that the effect of varied design parameters on the flow velocities of a cross-flow turbine can be determined. This based on the different CFD simulated results of nozzle openings. The variation in velocity distributions by the changes of varying inlet blade angles has identified. McGrattan *et al*. [20] have discussed that the simulated results of CFD analysis of fire flow by hydrodynamic model consists of the low Mach number large-eddy simulation helps to prevent protective systems in the buildings and structures.

Federico *et al*. [21] have explained that the condensation shock has anticipated the steam nodal location of the nozzle test case, whereas the steepness of the pressure rise in wet steam flow curves corresponds to the highlighted experiments. This condensation shock in the downstream region can be predicted by the average radius of the CFD simulation's various curves. Nadar *et al*. [22] and Haribabu *et al*. [23] utilized CFD technique and simulated the energy distribution in vortex and the flow of air in cars. Rajaguru *et al*. [24] reviewed on the various additive manufacturing technologies used for different applications. Maurya *et al*. [25] have experimentally verified the CFD simulation results of the stresses, strain, strain energy, and deformation of the journal bearing whether the equal pressure distribution has been occurred or not in the experimental part and they identified that the viscosity of the fluid film remains same that was not varied with respect the temperature. Water savings are such a challengeable task now a day which is not appropriately utilized by the people in the present scenario. Many flow control valves and reducers were discovered and used earlier to reduce water flow in the domestic appliances up to 80-90% in its flow rate.

In this research work, the holes are tiny in size and sensitively fabricated by 3-D printing based on the model obtained from the modeling tool Pro Creo. The acrylonitrile butadiene styrene (ABS) conventional thermoplastic polymers used for the fabrication of nozzle aerator. The flow rate can be determined based on the velocity distribution through each hole with uniform cross-sectional holes and the manufacture of this nozzle aerator by 3-D printing under the rapid manufacturing processes. Both ABS plastics can deliver the comparative results of the fabricated nozzle aerator, and the existing nozzle aerator is different based on the holes provided on it. The flow rate and velocity can reduce this if the cross-section of each hole will be very smooth and elegant. Product-based improvements have fulfilled the level of market demand.

Materials and methods

Research methodology

Based on the literature reviews and previous evidences, the procedures of research have been followed as mentioned in fig. 1. It begins with the problem identification followed by 3-D modelling and CFD analysis, 3-D fabrication of nozzle, and its assembly, with the co-ordination of pressure velocity prediction.
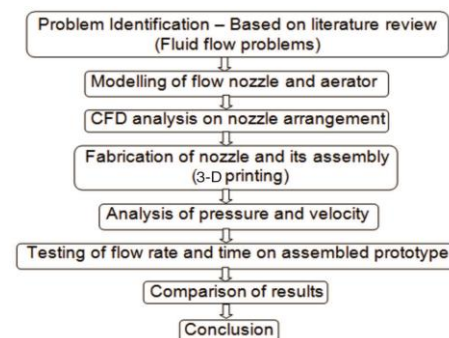
Figure 1. Research methodology process chart

Machine and material properties

The Envision TEC is a low-cost, open-architecture, easy to maintain, and user-friendly 3-D printer, as shown in fig. 2 used for a wide variety of professional and medical

collaborated applications. The Envision TEC boasts a high-resolution projector running at 1920×1080 pixel resolution with custom UV optics. Once the print job is pre-processed on a computer housing the Perfactory software suite, it transferred to the machine via Ethernet, Wi-Fi, or USB connection styles, and it can be run independently without the need for continuous connection to the pre-processing computer.

The following system properties should need for these 3-D printing processes. Compatible with leading dental, hearing aid, and other professional design software, any .stl file of a model designed from an impression or a scanner has printed as in fig. 3, it is capable of printing a wide variety of dental, orthodontic and hearing applications, changeover between materials is quick and easy with no waste. The touch screen and Wi-Fi capability enhance the user interface. Very few moving parts guarantee a strong and reliable production system. Out print ($L \times W \times H$): $39.5 \times 35.0 \times 82.55$ cm ($15.6 \times 13.8 \times 32.5$ in.) and weight 34 kg (75 lbs). The working conditions and the dimensions recovered from the regular usage of taps either used in 1 inch or 0.5 inch diameter pipelines. The nozzle aerator can be designed based on its dimensions. Applying complex shapes in its exit area, which contains minimal diameter fine holes, was provided by the hole cutting options in the design tool Creo as shown in fig. 4.

Figure 2. The 3-D printing machine Envision TEC

Figure 3. Front and backside view of the existing model and the newly fabricated nozzle aerator

Figure 4. Front and backside view of the newly developed model and fabricated nozzle aerator

862

Alphonse, B. H. B., *et al.*: Comparative Design and CFD Analysis of …
THERMAL SCIENCE: Year 2022, Vol. 26, No. 2A, pp. 857-869

Table1. Material and machine properties

Machine properties	
Name	Envision TEC
Build Envelope	$140 \times 79 \times 100$ mm ($5.5 \times 3.1 \times 3.95$ in.)
XY Resolution*	73 µm (0.0029 in.)
Dynamic Z Resolution	25 to 150 µm (0.001 to 0.006 in.) (*Material dependent)
Light Source	Industrial UV LED
Data Handling	STL
Material properties	
Name	ABS polymer
Type	Thermoplastic polymer
Material structure	Amorphous
Density	22-45 MPa
Thermal conductivity	0.14-0.21 W/mK
Tensile strength	28-55 MPa

Table 1 represents the machine properties of envision TEC having the interior capacity size and the material used for the 3-D printing of flow aerator. It comprises of LED light source with the peculiar data handling systems.

The ABS plastic is an ordinary thermoplastic polymer with high impact and chemical resistance with more structural strength and stiffness. It is having better performance in more upper and lower temperature applications. Initially, the availability of material and cost is good, and the rapid manufacturing applications use it. Using the patterning of holes, its count increased in both vertical and horizontal directions of its surface design. Thus the modeling has been fulfilled.

Similarly, the existing part can be developed by the same method with rectangular cross-sectional holes of non-uniform in size. This design has exported into the form .IGES or .stl for analysis in ANSYS Fluent. The working conditions and dimensions recovered from the regular usage of taps either used in 1 inch or 0.5 inch diameter pipelines. The nozzle aerator has designed for its dimensions. By applying complex shapes in its exit area, which contains a very small diameter with fine holes were provided by the hole cutting options in the design tool Creo as shown in fig.4.

By using the patterning of holes, its count increased is in both vertical and horizontal directions of its surface design. Similarly, the existing part can be developed by the same method with rectangular cross-sectional holes of no uniform in size. This design exported into the form of .IGES or .stl for analysis in ANSYS Fluent.

Experimental procedure

The CFD analysis and 3-D printing

The CFD is the computer's application to defer the information regarding the fluid-flow characters and the flow regulations. The CFD analysis can easily identify the liquid flow behavior through any required modern tool usage. These advanced tools can easily capture the pressure, velocity and flow rates. The input and output pressures have been indicated with the values of Pascal with the relative momentum of respective Z-axis components of flow direction has represented in the fig. 5.

Accordingly, these methods have evolved mutually with the technology adopted in computers and thus find their beginnings some more years ago. The CFD methods are inimitable in simultaneously using several techniques such as mathematics, computer science, engineering, and physics to model the fluid-flows.

Alphonse, B. H. B., *et al.*: Comparative Design and CFD Analysis of …
THERMAL SCIENCE: Year 2022, Vol. 26, No. 2A, pp. 857-869

863
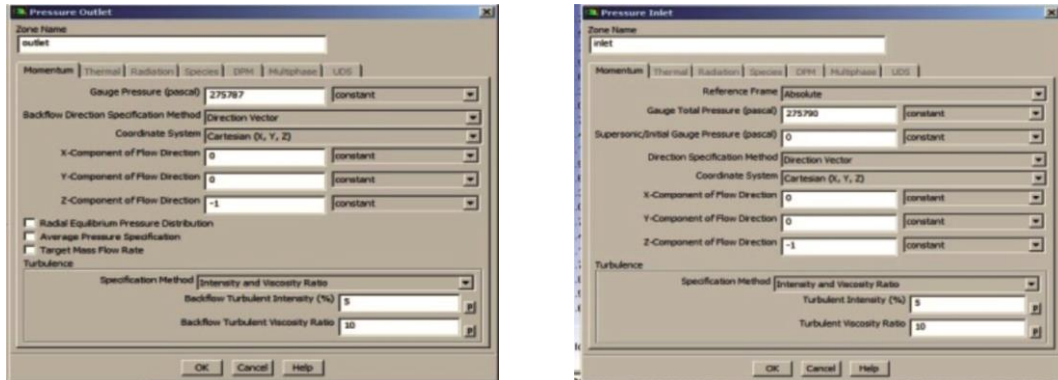
Figure 5. Initial and final pressure used for CFD analysis

In this research project, ANSYS Fluent has adopted the development of CFD simulation results among this newly fabricated nozzle aerator. The simulation results confirmed that the pressure distribution could be a uniform based on the cross-section of the nozzle aerator screwed with the main pipe, as shown in fig. 6. The velocity distribution has varied with respect to the fine holes provided at the outer surface of the nozzle aerator, as mentioned in fig. 7. The holes and the components can be fabricated by 3-D printing because it is very
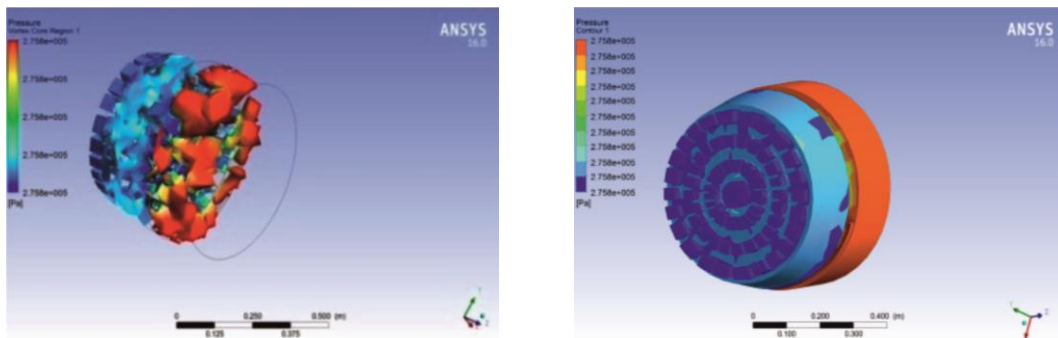
Figure 6. The CFD simulation results of pressure distribution in Nozzle 1

complicated by the common conventional type of fabrications. Figure 8 showed that its precise finishing differentiates the size and the beautiful edges of the existing and fabricated new nozzle aerator by 3-D printing technology. Especially with cute holes, these simulation procedures and outcomes are valuable only for the level of prediction of fluid-flow analysis for real-time applications.
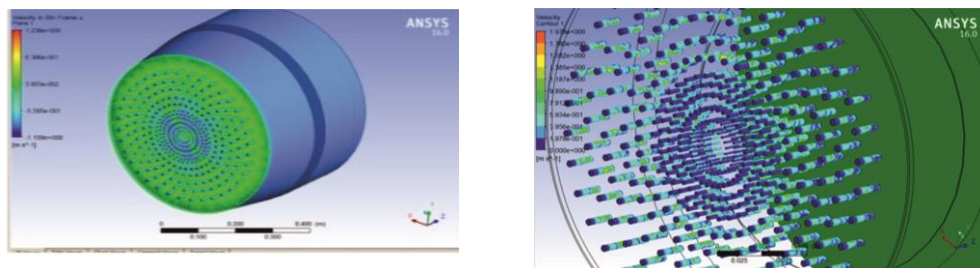
Figure 7. The CFD simulation results of the velocity distribution in Nozzle 2
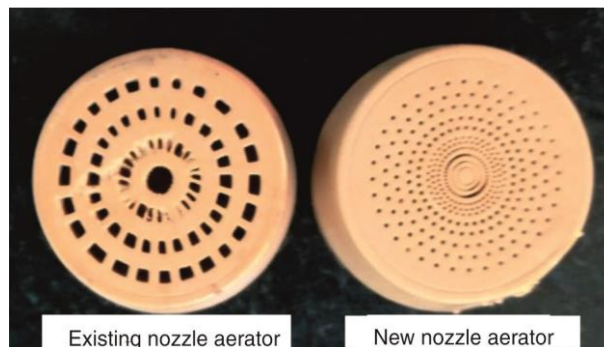
Figure 8. The fabricated nozzle aerators

Determination of flow rate of nozzle aerator front side

The flow rate can be defined as a discharge of water at any outlet by considering the mass of water flowing concerning time duration. In the first case of discharge calculations, the flow rates can be calculated based on the N number of fine holes provided at the front side of the nozzle aerator, which attains the water-saving principles. The fine holes of the same side have supplied in the single circulatory direction to its axis. Similarly, the fine holes of different diameters can be provided over the concentric circular cross-sections, as shown below in fig. 9.
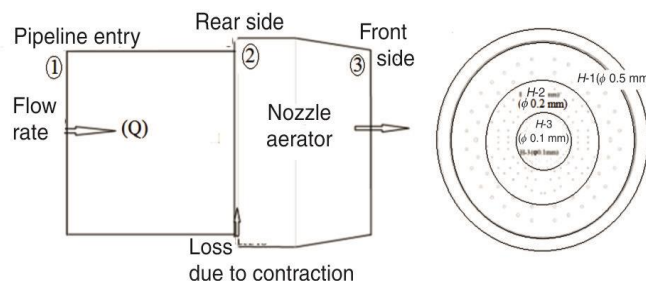
Figure 9. Holes at the backside of the nozzle aerator for various diameters

Let consider the flow rate as Q and N are the numbers of fine holes. Here, the usage of 1 inch and 0.5 inch pipes adopted for the flow analysis using the newly introduced 3-D printed nozzle aerator attached in the tap assembly. Here the flow rate can be considered as Q, and the number of fine holes provided in 3-D model nozzle aerator becomes N, and the discharge of one small hole has mentioned as Q_x.

If the diameters of the fine holes are same the discharge can be given as $Q = N_1Q_1$.

If the holes are in different size and numbers, $Q = \sum N_x Q_x$.

The summation of flow rates among three cross-sections can be calculated based on its diameters. The uniform velocity has maintained for the entire fluid-flow processes. Based on design considerations and flow properties, $Q = N_1Q_1$, where, $i = 1,2,3,…$

For the first circumference, $N_1Q_1 = 40Q_1$, $N_2Q_2 = 40Q_2$ and $N_3Q_3 = 40Q_3$.

The calculated value and the summation of the flow rate $Q = Q_1 + Q_2 + Q_3$ can be calculated and verified as 0.036 L per second.

Determination of flow rate from the rear side of the nozzle aerator

The water has supplied from the rear side of the nozzle aerator with three different assumptions based on its backside opening diameters of the nozzle aerator, as mentioned in fig. 10. By considering the flow of water, the tank to the pipeline has maintained the final pressure of P1 and the uniform velocity of 2.5 m/s.
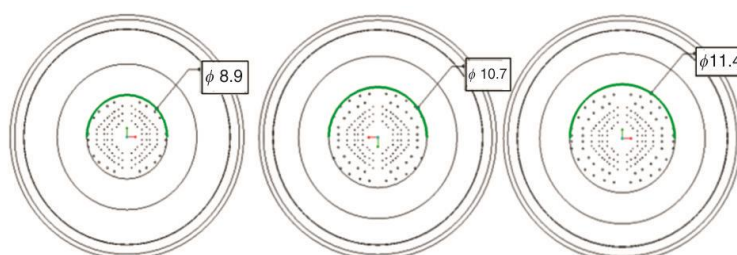
Figure 10. Fine holes of diameters 11.4 mm, 10.7 mm, and 8.9 mm provided at the back side of the nozzle aerator

The loss function has initiated due to sudden contraction from the tap area to the nozzle aerator entry because of the reduction in diameters of aerator rear side entry from the pipeline. By using the reduction of loss due to sudden contraction is mentioned by:

$$Q = A_1 V_1 \quad \text{and} \quad Q = A_2 V_2 \tag{1}$$

where V is the velocity of flow, g – the force due to gravity, and h_c – the contraction loss in the pipeline.

$$\frac{P_1}{\rho g} + \frac{V_1^2}{2g} + Z_1 = \frac{P_2}{\rho g} + \frac{V_2^2}{2g} + Z_2 + \text{Contraction Loss} \tag{2}$$

The highlighted observations of pressure, velocities of the existing nozzle, and the newly developed nozzle have received by solving the aforementioned eqs. (1) and (2). In this case, along the aerator's rear side, the fine holes are to be converted into a though all holes up to its extended lengths at its rear side. The variation in its diameter has been recommended and determines the different discharge values concerning uniform velocity. By adding all the flow rates which are having different in diameters of 11.4 mm, 10.7 mm, and 8.9 mm becomes:

$$Q_{avg} = \sum QA$$

By this method of calculation, we got an average value of discharge $Q_{avg} = 0.2118$ L per seconds of the flow through the rear side due to reduced cross-sectional diameters.

Pressure and velocity findings for Nozzle 1

The volume of water flowing with respect to time for the discharge of the water through the pipeline is defined by:

$$Q = A_1 V_1 \quad \text{and} \quad Q = A_2 V_2 \tag{3}$$

The pipe of diameter 12.7 mm as D_1 and area of cross-section $A_1 = 0.000126$ m^2 with the maximum velocity of tap water V_1 as 2.5 m/s. The discharge value of the flow rate,

866

Alphonse, B. H. B., *et al.*: Comparative Design and CFD Analysis of …
THERMAL SCIENCE: Year 2022, Vol. 26, No. 2A, pp. 857-869

Q, was calculated as 0.000316 m^3/s. Similarly, for the pipe of diameter D_2 of 11.4 mm of the area A_2 is 0.000102 m^2, the following procedure can calculate the corresponding value of tap water velocity, $0.000316 = 0.000102V_2$ then, we get the exit velocity V_2 of 3.09 m/s.

By applying Bernoulli's equation, with neglecting of datum heads, the pressure at the inlet of the pipe $P_1 = 275790.3$ Pa (typical inlet water pressure to a home):

$$\frac{P_1}{\rho g} + \frac{V_1^2}{2g} + Z_1 = \frac{P_2}{\rho g} + \frac{V_2^2}{2g} + Z_2 \tag{4}$$

$$P_1 + V_1^2 = P_2 + V_2^2 \tag{5}$$

By substituting the values in the mentioned eq. (5), $275790.3 + 2.52 = P_2 + 3.092$, then we get the pressure values at Section 2 as $P_2 = 275787.002$ Pa.

Similarly for the different diameters 11.4 mm, 10.7 mm, and 8.9 mm at its rear side of the nozzle aerator as shown in fig. 10 the flow rate becomes:

$Q_1 = 2.552 \cdot 10^{-4}$ m^3/s, $Q_2 = 2.248 \cdot 10^{-4}$ m^3/s, and $Q_3 = 1.553 \cdot 10^{-4}$ m^3/s.

It is noted that the rear side arrangements are common for both existing and new nozzles. The changes in its front side of the nozzle only gave good results of flow characteristics.

Pressure and velocity findings for Nozzle 2

The similar steps can be followed for the nozzle aerator 2 of having velocity and diameters of $V_1 = 2.5$ m/s, $D_1 = 12.7$ mm we get $P_1 = 275290.3$ Pa and the values at the exit of the nozzle for the diameter of $D_2 = 11.4$ mm, we get $P_1 = 275290.3$ Pa (water pressure of 1/2 inch tap).

Let the solution can be modified for 40 holes, $A_{40} = 7.856 \cdot 10^{-6}$ m^2, $A_2 - A_{40} = 1.0207 \cdot 10^{-4} - 7.856 \cdot 10^{-6}$ and we get, $A_{\text{remaining}} = 0.0001018$ m^2.

The outlet area can be calculated by the following method:

$$A_{\text{outlet}} = A_2 - A_{\text{remaining}} = 1.0207 \cdot 10^{-4} - 0.0001018$$

we get, $A_2 = 8.264 \cdot 10^{-7}$ m^2.

The discharge or flow rate can be calculated for the determined values of each area of cross sections:

$$Q_1 = A_1 V_1 = 1.266 \cdot 10^{-4} \times 2.5$$

we get, $Q_1 = 0.0003165$ m^3/s

Here we assume that $Q_1 = Q_2 = 0.0003165$ m^3/s.

By using the value of discharge, the velocity can be calculated as:

$Q_2 = A_2 V_2 = 8.264 \cdot 10^{-7} \times V_2 = 0.0003165 V_2 = 0.0003165/(8.264 \cdot 10^{-7}) V_2 = 3.82$ m/s

Applying the Bernoulli's equation procedure of (4), by assuming the datum heads $Z_1 = Z$ and it becomes:

$$P_1 + V_1^2 = P_2 + V_2^2 \quad \text{and we get } P_2 = 275767 \text{ Pa}$$

Results and discussion

By identifying the summation of flow rates of Q_1, Q_2, and Q_3, it can confirm its safe design based on its cross-sections of each hole to satisfy the water-saving principles; similarly, by the flow rate value Q_1, the laminar flow has been obtained based on its Reynolds number of 356.74 which is less than 2000. Meanwhile, the turbulent flow might be initiated by the reduction of the cross-sectional area present in the nozzle rear and front side, respectively. The decrease of nozzle aerator cross-sections happened in the turbulent flow.

Alphonse, B. H. B., *et al.*: Comparative Design and CFD Analysis of …
THERMAL SCIENCE: Year 2022, Vol. 26, No. 2A, pp. 857-869

867

Based on the findings of flow rate, pressure, and velocity, the values of pressure mentioned in tab. 2 have reduced for various nozzle designs. The primary pipeline pressure could be much higher compare with the Nozzles 1 and 2. Similarly, the tremendous improvements have been obtained by the velocity values by the Nozzle Aerators 1 and 2 compare with the main pipeline, as shown in tab. 3.

Table 2. Pressure and velocity observations from the experimentations

Parameters	Pipe line	Nozzle 1	Nozzle 2	Calculated with a loss function
Pressure [Pa]	275790.3	275787	275767	275656.095
Velocity [ms^{-1}]	2.5	3.09	3.82	3.79

Table 3. The difference of nozzle aerator flow rate in the rear and front side

	Front side of the nozzle aerator	Rear side of the nozzle aerator
Flow rate	$3.6 \cdot 10^{-5}$ m^3 per seconds or 0.036 L per seconds	$2.118 \cdot 10^{-4}$ m^3 per seconds or 0.2118 L per seconds

The high velocity of 3.82 m/s can be obtained by the Nozzle Aerator 2. Here the minor loss function was applied and indicated in the form of loss due to sudden contraction. The head loss has considered a minor loss, and the velocity has been increased more compare with the nozzle one and the main pipeline. The observations of pressure and velocities have shown in fig. 11.
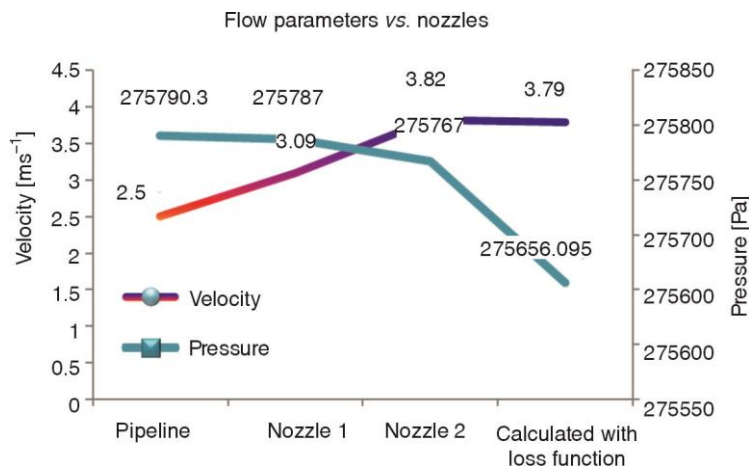
Figure 11. Observations of flow parameters and nozzle arrangements

Easy prediction by the ANSYS Fluent software tool, the CFD analysis results has carried out, as shown in fig. 7. The solid modeling of nozzle aerators is used for the CFD analysis. The water particles uniformly distribute the flow through the small holes of the nozzle aerator. Comparatively, in the existing nozzle aerator, the flow exit patterns are plentiful, and the flow is non-uniform or irregular. These observations will lead to massive consumption of water through these large dimensional cross-sections.

These simulated results of ANSYS Fluent can be compared with the testing images of the flow of water with the water tap assembly, as shown in figs.12(a)-12(d). It is evident

868

Alphonse, B. H. B., *et al.*: Comparative Design and CFD Analysis of …
THERMAL SCIENCE: Year 2022, Vol. 26, No. 2A, pp. 857-869

that the narrow stream of water can be evenly expelled out from the nozzle aerator outlet with optimum time duration, which has been provided with these fine shaped holes of the tap assembly even though it has unevenly distributed from the existing nozzle aerator. Thus the consumption of water usage can be reduced compared with the existing nozzle aerators.

(a)   (b)   (c)   (d)

Figure 12. Difference in flow outcome by; (a) and (b) existing nozzle aerator and (c) and (d) new nozzle aerator

Conclusion

In this fluid research project, the flow rate has minimized by replacing newly developed nozzle aerators in the water tap assembly used for domestic purposes. The rapid prototype of this nozzle aerator design has produced by the 3-D printing method for quick and precise fabrication of the specimen sample. The accurate design calculations have made to avoid the misalignment of nozzle aerator with the tap assembly. The reduction of pressure and velocity indicated the flow calculations could be reduced gradually with the decrease in cross-sectional changes in its design. The number of fine holes provided in the face of the nozzle aerator makes the flow becomes very smooth. Meanwhile, economically the water can be saved up to 39.14% by the involvement of newly developed nozzle aerators. These measurements and methodologies which has followed here have utilized for different flow applications, either product development or study of fluid-flow characteristics through different geometric structures. Furthermore, the effective design and rapid manufacturing of the smooth fluid-flow deliverance products will be developed for the public as future scope.

Nomenclature

A_1, A_2, A_3 – area of the cross-section at different sections 1, 2, and 3 [m²]
D – diameter [m]
IGES – initial graphics exchange specification
L – length [m]
N_1, N_2, N_3 – number of fine holes in the nozzle aerator at different sections 1, 2, and 3

P_1, P_2, P_3 – pressure of water flow at different sections 1, 2, and 3 [Pa]
Q_1, Q_2, Q_3 – flow rate of water at different sections 1, 2, and 3 [m³ per second]
STL – stereo lithography
V_1, V_2, V_3 – velocity of water at different sections 1, 2, and 3 [ms⁻¹]
Z – datum heads

References

[1] Rahi, K. H*., et al.,* Experimental and Numerical Analysis of Flow through Pipe for Different Geometry, *Proceedings*, Int. Con. on Mechanical, Industrial and Energy Engineering, Dhaka, Bangladesh, 2016

Alphonse, B. H. B., *et al.*: Comparative Design and CFD Analysis of …
THERMAL SCIENCE: Year 2022, Vol. 26, No. 2A, pp. 857-869

869

[2]   Pandey, K. M., CFD Analysis of Flow through Compressor Cascade, *International Journal of Soft Computing and Engineering*, *2* (2012),1, pp. 362-371
[3]   Liu, H., *et al.*, Analytical Equation for Outflow Along the Flow in a Perforated Fluid Distribution Pipe. *PLOS ONE*, *12* (2017), 10, pp. 1-8
[4]   Baghdadi, A. H. A., Mansy, H. A., A Mathematical Model for Leak Location in Pipelines, *Applied Mathematical Modelling*, *12* (1988), Feb., pp. 25-30
[5]   Pradeep Mohan Kumar, K., *et al.*, Computational Analysis and Optimization of Spiral Plate Heat Exchanger, *J. of Applied Fluid Mechanics, 11 (2018),* Special issue, pp. 121-128
[6]   Tartibu, L.K., Kunene, T., Numerical Analysis of the Flow Pathlines in Thermo-Acoustic Couples, *Procedia Manufacturing*, *35* (2019), pp. 246-251
[7]   Farsirotou, E., *et al.*, Experimental Investigation of Fluid-Flow in Horizontal Pipes System of Various Cross-Section Geometries, *EPJ Web of Conferences*, *67* (2014), Mar., pp. 1-4
[8]   Vijayan, V., *et al.*, CFD Modeling and Analysis of a Two-Phase Vapor Separator, *Journal of Thermal Analysis and Calorimetry, 145* (2020), May, pp. 2719-2726
[9]   Adel, M., *et al.*, A Comparative Study of Impeller Aerators Configurations, *Alexandria Engineering Journal, 58* (2019), 4, pp. 1431-1438
[10] Wang, W., *et al.*, Analysis of Laminar Flow and Heat Transfer in an Interrupted Micro Channel Heat Sink with Different Shaped Ribs, *J. of Thermal Analysis and Calorimetry*, *140* (2020), pp. 1259-1266
[11] Shukla, B.K., Goel, A., Study on Oxygen Transfer by Solid Jet Aerator with Multiple Openings, *Engineering Science and Technology, An International Journal*, *21* (2018), 2, pp. 255-260
[12] Jahan, S.A., *et.al.*, Implementation of Conformal Cooling & Topology Optimization in 3D Printed Stainless Steel Porous Structure Injection Molds, *Procedia Manufacturing*, *5* (2016), Dec., pp. 901-915
[13] Kamel, M. S, Simulation of Pool Boiling of Nanofluids by Using Eulerian Multiphase Model, *Journal of Thermal Analysis and Calorimetry*, *142* (2019), Dec., pp. 493-505
[14] Jafari, D., *et al.*, Metal 3D-printed Wick Structures for Heat Pipe Application: Capillary Performance Analysis, *Applied Thermal Engineering*, *143* (2018), Oct., pp. 403-414
[15] Lorinczy, D., *et al.*, Differential Thermal Analysis of the Antibacterial Effect of PLA-Based Materials Planned for 3D Printing, *Journal of Thermal Analysis and Calorimetry, 139* (2020), pp. 367-374
[16] Naresh, B., *et al.*, Design and Analysis of Mixed Flow Pump Impeller, *International Journal of Trend in Scientific Research and Development*, *3* (2019), 3, pp. 1180-1184
[17] Guo, H., *et al.*, Recent Advances in 3D Printing Graphene-Based Composites, *Nano Material Science, 1* (2019), 2, pp 101-115
[18] Kumar, M., *et al.*, Design and Numerical Investigation to Visualize the Fluid-Flow and Thermal Characteristics of Non-Axisymmetric Convergent Nozzle, *Engineering Science and Technology, An International Journal*, *22* (2019), 1, pp. 294-312
[19] Bhowmick, S., *et al.*, A Simulation Based Study of flow Velocities Across Cross Flow Turbine at Different Nozzle Openings, *Procedia Technology, 25* (2016), pp. 974-981
[20] McGrattan, K., *et al.*, Computational Fluid Dynamics Modelling of Fire, *International Journal of Computational Fluid Dynamics*, *26* (2012), 6-8, pp. 349-361
[21] Federico, M., *et al.*, CFD Modelling of the Condensation Inside a Supersonic Nozzle: Implementing Customized Wet-Steam Model in Commercial Codes, *Energy Procedia, 126* (2017), Sept., pp. 34-41
[22] Nader, P., *et al.*, Computational Fluid Dynamics Analysis of Helical Nozzles Effects on the Energy Separation in a Vortex Tube, *Thermal Science*, *16* (2012), 1, pp. 151-156
[23] Haribabu, K., *et al.*, Investigation of air Conditioning Temperature Variation by Modifying the Structure of Passenger Car Using Computational Fluid Dynamics, *Thermal Science*, *24* (2020), 1B, pp. 495-498
[24] Rajaguru, K., *et al.*, Additive Manufacturing – State of art, *Materials Today Proceeding, 21* (2020), 1, 2020, pp. 628-633
[25] Maurya, A., *et al.*, CFD and Frictional Torque Analysis of Hydrodynamic Journal Bearing", *International Journal of Engineering Research and Technology, 8* (2019), 7, pp 959-968